Direct Measurement of Poloidal Long-Wavelength $E \times B$ Flows in the HT-7 Tokamak

G. S. Xu, B. N. Wan, M. Song, and J. Li

Institute of Plasma Physics, Chinese Academy of Sciences, Hefei, People's Republic of China

(Received 24 January 2003; published 16 September 2003)

The poloidal long-wavelength $E \times B$ time-varying flows were directly measured using a forked Langmuir probe in the HT-7 tokamak. Low-frequency (<10 kHz) $E \times B$ flows were observed at the plasma edge, which possess many of the characteristics of zonal flows, including a poloidal long-wavelength ($k_\theta \rho_i \sim 0$) and narrow radial extent ($k_r \rho_i \sim 0.1$). The cross bicoherence of turbulent Reynolds stress indicates the existence of nonlinear three-wave coupling processes and the generation of low-frequency $E \times B$ flows. The estimated flow-shearing rate is of the same order of magnitude as the turbulence decorrelation rate and may thus regulate the fluctuation level and thereby the turbulence-driven transport.

DOI: 10.1103/PhysRevLett.91.125001 PACS numbers: 52.35.Ra, 52.25.Fi, 52.55.Fa

It is generally accepted that anomalous transport in magnetized fusion plasmas is due to microturbulence. Recent progress in understanding the formation of a transport barrier in fusion plasmas reemphasized the importance of turbulence-driven flows via Reynolds stress (RS) [1]. Since shear flows suppress turbulence through the shear decorrelation mechanism [2], it is expected that the flows/turbulence dynamics controls the fluctuation level and, as a result, affects the turbulent transport. Recent theoretical work indicates that plasma turbulence may exist in a self-regulated state mediated by zonal flows (ZF) [3], which are toroidally and poloidally symmetric and radially localized potential perturbations. Such perturbations are spontaneously generated by ambient turbulence (AT) via the action of RS and can be described as low-frequency poloidal long-wavelength $E \times B$ flows [4]. The theoretical effort supported by simulations [5] and several suggestions on the manifestation of ZF in experiments has been proposed [6,7].

Given the great significance attributed to the ZF in establishing the turbulence self-regulation dynamics, there is considerable interest in observing the features of ZF in fusion plasmas. Several experiments until now have identified some of the features of ZF in tokamak edge plasmas [8–12]. Since ZF are essentially potential structure, which occur mainly in the poloidal $E \times B$ flows and are generally expected to be manifested less strongly in the density field (i.e., $\tilde{n}/n < e\tilde{\phi}/T_e$), the direct experimental evidence of such flows requires the direct measurement of the poloidal large-scale $E \times B$ flows. However, experiments addressing this problem until now have examined only the features of density turbulence [9,12]. The only potential measurements related to this topic were conducted in low-temperature heliac plasmas [13], where turbulence was not completely developed and narrow band fluctuations dominated the spectra. The theory predicted broad band (0–10 kHz) ZF eigenmode and its generation process are still absent of observation. In this Letter, we report the first direct measurement of poloidal long-wavelength $E \times B$ flows in the tokamak edge plasmas.

HT-7 is a superconducting tokamak with two circular poloidal limiters toroidally separated by 180° and a high-field-side belt limiter. This experiment was conducted in Ohmic heated deuterium plasmas ($R_0 = 122$ cm, $a = 27$ cm, $B_\phi \cong 1.8$ T, $I_p \cong 100$ kA, $\bar{n}_e \cong 1.5 \times 10^{19}$ m^{-3}, $T_{e0} \cong 0.5$ keV, $n_{\text{e-edge}} \cong (1.5\text{–}4) \times 10^{18}$ m^{-3}, $T_{\text{e-edge}} \cong 40\text{–}120$ eV, and discharge duration $\cong 1$ s). These parameters were specially selected because, in such low parameter discharges, the edge safety factor $q_a > 5$ and there was no sawtooth and very little magnetohydrodynamic activity. The poloidal correlation length $L_{c\theta}$ of turbulence at the plasma edge is normally close to 1 cm, so that, to achieve the measurement of poloidal large-scale $E \times B$ flows, a specially designed Langmuir probe (see Fig. 1) was used, with two probe heads poloidally separated by 31.4 mm, which was much longer than the $L_{c\theta}$. On each of the two heads a triple tips array was used to provide local measurement of the radial electric field E_r and electrostatic RS $\langle \tilde{V}_r \tilde{V}_\theta \rangle$ [14], where $\langle \cdots \rangle$ denotes

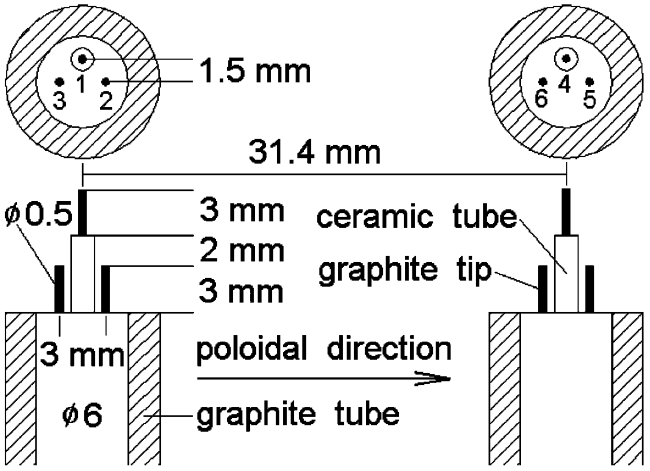

FIG. 1. Structure of the forked probe.

an ensemble average. All tips were used to measure floating potential ($\phi_{f1}, f_{f2}, \ldots, \phi_{f6}$). Then the radial and poloidal E_r fluctuations can be calculated as $\tilde{E}_{r1} = (\tilde{\phi}_{f1} - \tilde{\phi}_{23})/\delta_r$ and $\tilde{E}_{\theta 1} = (\tilde{\phi}_{f2} - \tilde{\phi}_{f3})/\delta_\theta$, neglecting the contribution from electron temperature [8,15,16], where $\tilde{\phi}_{23} = (\tilde{\phi}_{f2} + \tilde{\phi}_{f3})/2$. Thus, the poloidal and radial $E \times B$ flows are calculated as $\tilde{V}_{\theta 1} = \tilde{E}_{r1}/B_\phi$ and $\tilde{V}_{r1} = \tilde{E}_{\theta 1}/B_\phi$. Similarly, the triple tips on the right probe head give $\tilde{V}_{\theta 2} = \tilde{E}_{r2}/B_\phi$. The probe was mounted on the top of the tokamak along the central line and operated with shot-to-shot scanning. Feedback control of the plasma position ensured that the two heads were located on the same magnetic flux surface. Both the probe tips and the shield tubes were made of graphite to allow the reliable measurement 2.5 cm inside the last closed flux surface (LCFS). The data was sampled at 1 MHz with 12-bit resolution using a multichannel digitizer. The boundary profiles of plasma parameters were measured with a fast reciprocating Langmuir probe [17] using a standard triple tips array. All measurements were done in the laboratory frame.

High resolution of the poloidal wave number ($-1 < k_\theta < 1$ rad/cm) can be achieved using this forked probe, so that small k_θ components of poloidal $E \times B$ flows can be distinguished from the AT. Application of this method to discern the large-scale flows requires that the lifetime of AT eddies is shorter than the transit time of turbulence eddies across the long distance. This condition is satisfied for the specially designed probe. The decorrelation time of floating potential fluctuations at the plasma edge is about $t_c \cong 8$ μs. The equilibrium flow velocity is about 2 km/s [16], resulting in a 16 μs transit time τ_d across the 31.4 mm spatial separation, so that $\tau_c < \tau_d$. The ZF are expected to correlate between two points with long poloidal space, while the correlation in AT will decay with the increase of distance. Therefore using the two-point correlation method between the two probe heads, separated by 3.14 cm, the coherent low-frequency flows can be extracted from background fluctuations.

The standard two-point correlation technique [18] was applied to the two probe signals $\tilde{V}_{\theta 1}$ and $\tilde{V}_{\theta 2}$. The spectra displayed in Fig. 2 were measured at the LCFS ($\Delta r = 0$). As shown in Fig. 2(a), the auto power spectrum of $\tilde{V}_{\theta 1}$ exhibits the typical broad band (0–100 kHz) feature. Figures 2(b) and 2(c) show the cross power spectrum and coherency (correlation coefficient) spectrum between $\tilde{V}_{\theta 1}$and $\tilde{V}_{\theta 2}$, respectively. Although the space between the two probe heads was much longer than the $L_{c\theta}$ [19], there was still considerable coherency of the AT, which implies the AT contains many long life components at a time scale much longer than the lifetime of turbulence eddy (10 μs). This phenomenon of plasma turbulence has recently become the subject of intense interest and investigation in plasma physics [20]. Recent experiments on different devices [21] demonstrated the existence of long-range correlations and self-similarity in plasma fluctuations at time scale 0.01–10 ms, which implies long life events

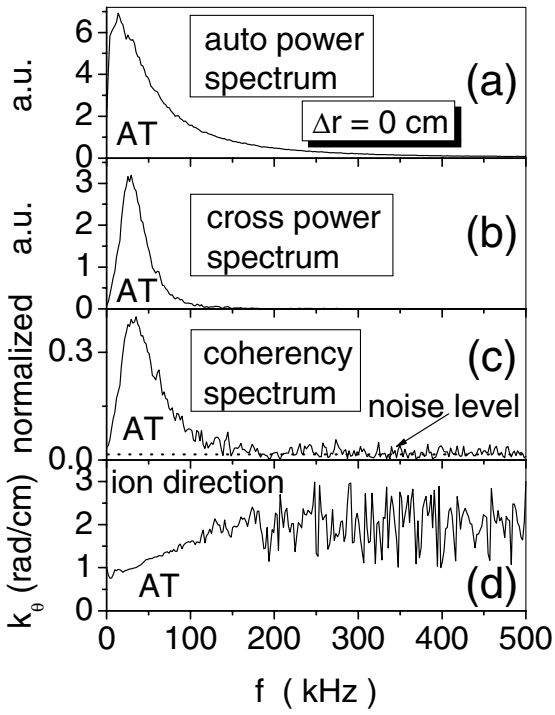

FIG. 2. Spectra measured at the LCFS ($\Delta r = 0$). (a) Auto power spectrum of $\tilde{V}_{\theta 1}$. (b) Cross power spectrum. (c) Coherency spectrum. (d) Poloidal wave number spectrum. (b), (c), and (d) were calculated from the long distance correlation between $\tilde{V}_{\theta 1}$ and $\tilde{V}_{\theta 2}$.

contributing significantly to turbulent transport is possibly a universal phenomenon in fusion plasmas. The experimental results presented here give good evidence for the existence of long-range correlations of the AT. No low-frequency coherent structure can be found at this radial location. The spectra measured in the SOL have the similar features as that at the LCFS. A possible reason is that the flow lines on one magnetic flux surface were cut off by the limiters and the ZF cannot exist in this region. The k_θ spectrum [Fig. 2(d)] indicates that at this radial location the AT propagated in the ion diamagnetic drift direction and the averaged k_θ is about 1 rad/cm. As shown in this figure, no $k_\theta \sim 0$ fluctuation component can be found in the low-frequency region.

When the probe was inserted across the LCFS, the spectrum features were quite different from that in the SOL, as displayed in Fig. 3 ($\Delta r = -2.1$ cm). In the auto power spectrum of $\tilde{V}_{\theta 1}$ [Fig. 3(a)], the spectrum peak of AT moves to the higher frequency region (about 62 kHz) and a broad band low-frequency component (0–25 kHz) appears. With the long distance correlation method, the low-frequency $E \times B$ flows emerge, as shown in Figs. 3(b) and 3(c). A broad band (0–10 kHz) low-frequency coherent mode can be clearly seen and is well above the noise level. The coherence spectrum was calculated from 1170 realizations (mean removed) of 512 samples and the noise level was determined from the coherence level at close to 500 kHz. The k_θ of this low-frequency mode is about zero,

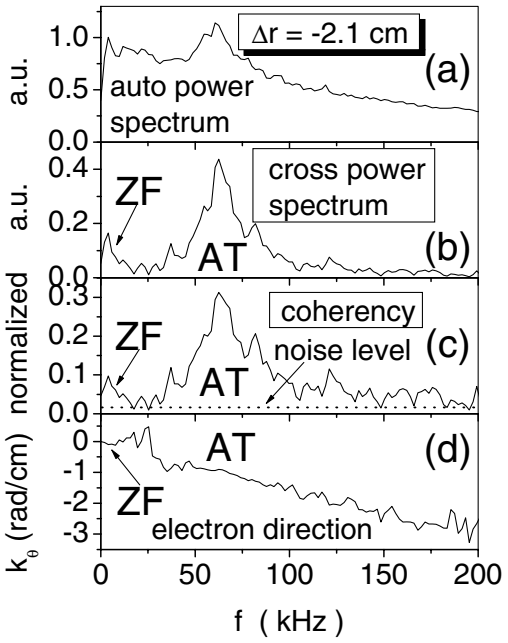

FIG. 3. Spectra measured at the plasma edge ($\Delta r = -2.1$ cm). (a) Auto power spectrum of $\tilde{V}_{\theta 1}$. (b) Cross power spectrum. (c) Coherency spectrum. (d) Poloidal wave number spectrum. (b), (c), and (d) were calculated from the long distance correlation between $\tilde{V}_{\theta 1}$ and $\tilde{V}_{\theta 2}$.

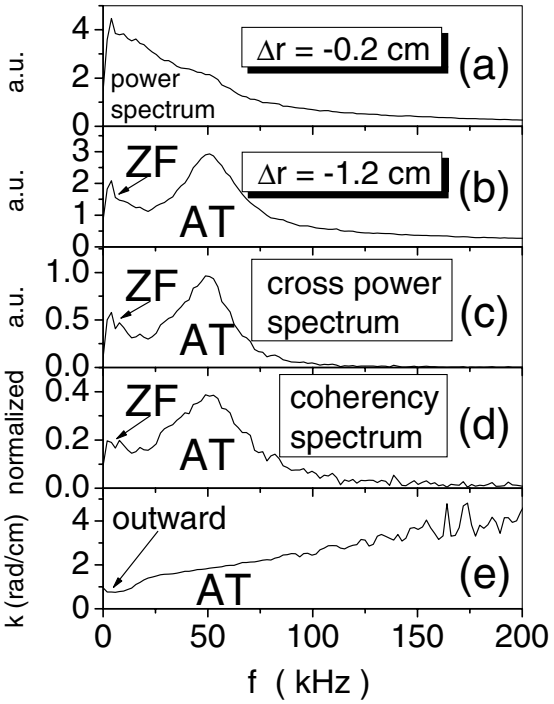

FIG. 4. Spectra measured with the modified forked probe. (a) Auto power spectrum of $\tilde{V}_{\theta 1}$ ($\Delta r = -0.2$ cm). (b) Auto power spectrum of $\tilde{V}_{\theta 2}$ ($\Delta r = -1.2$ cm). (c) Cross power spectrum. (d) Coherency spectrum. (e) Wave number spectrum. (c), (d). and (e) were calculated from the long distance correlation between $\tilde{V}_{\theta 1}$ and $\tilde{V}_{\theta 2}$.

as shown in Fig. 3(d). For the high-frequency AT, its k_θ spectrum displays obvious characteristics of the drift wave and its average k_θ is close to -1 rad/cm, where negative means propagating in the electron diamagnetic drift direction.

To measure the radial wave number k_r of this low-frequency mode, one probe head was made 1 cm longer than the other one, so the two probe heads were not only poloidally separated by 31.4 mm but also radially separated by 10 mm. Through the long distance correlation between $\tilde{V}_{\theta 1}$ and $\tilde{V}_{\theta 2}$, the wave number $\vec{k} = \vec{k}_\theta + \vec{k}_r$ with two components was obtained. Since the k_θ of this low-frequency mode is about zero, its k_r can be approximately estimated as $k_r \cong k$. Figures 4(a) and 4(b) show the auto power spectra of $\tilde{V}_{\theta 1}$ ($\Delta r = -0.2$ cm) and $\tilde{V}_{\theta 2}$ ($\Delta r = -1.2$ cm), respectively. For the probe head deep into the plasma edge, its spectrum has two components; one high-frequency AT component peaks at around 50 kHz and one low-frequency broad band component has a frequency width about 20 kHz. For the probe head just 2 mm inside the LCFS, its spectrum has only one component and the low-frequency mode is submerged in the AT. Figures 4(c) and 4(d) indicate that two components exist in the $E \times B$ flow fluctuations. From the long distance correlation k spectrum [Fig. 4(e)], we get the estimated k_r of the low-frequency mode as 0.8 rad/cm. If we presume the ion temperature $T_i \cong T_e$, then we can calculate the ion gyroradius as $\rho_i \cong 0.7$–1.2 mm and $k_r \rho_i \cong 0.06$–0.1. In this paper, before calculating these spectra, the mean value has been removed from every time realization (0.5 ms), so the equilibrium flow (time scale longer than 0.5 ms) was not included in these spectra.

The root-mean-square (rms) amplitude of the low-frequency $E \times B$ flows, normalized to the ion thermal velocity ($V_{\mathrm{Ti}} \cong 44$–76 km/s) is $\tilde{V}_\theta^{\mathrm{ZF}}/\mathrm{V_{Ti}} \cong 0.5\%$–$0.9\%$ at the plasma edge. For comparison, the rms value of the ambient turbulent flows, normalized to V_{Ti} is $\tilde{V}_\theta^{\mathrm{AT}}/\mathrm{V_{Ti}} \cong 1.6\%$–$2.7\%$. The rms magnitude of the low-frequency $E \times B$ flows can be used to infer a turbulence shearing rate due to the finite k_r of this poloidal flow structure. Taking the shearing rate to be approximately $\omega_s = d\tilde{V}_\theta/dr = 2\tilde{V}_\theta^{pp}/\lambda_r$, where λ_r is the radial wavelength and $\tilde{V}_\theta^{pp}$ is the peak-to-peak value of the low-frequency $E \times B$ flows, we find $\omega_s \cong 3 \times 10^4\ \mathrm{s}^{-1}$. This is comparable to the decorrelation rate of the floating potential fluctuations $\gamma \sim 12 \times 10^4\ \mathrm{s}^{-1}$, which is calculated as the inverse of the decorrelation time. The equilibrium flow shear rate at the same measurement point is calculated as $\omega_s \sim 7 \times 10^4\ \mathrm{s}^{-1}$. The estimated fluctuating flow-shearing rate is thus of the same order of magnitude as the equilibrium flow shear rate, suggesting that the time-varying flows and equilibrium flow are both important to stabilize the turbulence. Since the flow shear is not strong enough to completely suppress turbulence, a naturally occurring weak transport barrier existed at the plasma edge, which resulted in a steeper pressure profile; however, the confinement is still low and falls into

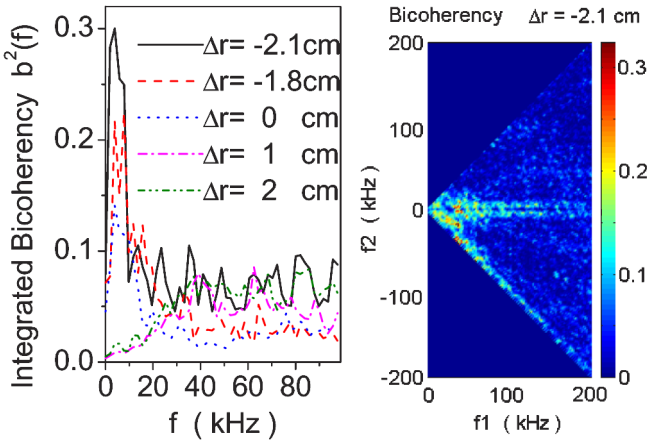

FIG. 5 (color online). (left panel) Spectra of integrated bicoherency $b^2(f) = \sum_{f=f_1+f_2}\langle \tilde{V}_r(f_1)\tilde{V}_\theta(f_2)\tilde{V}^*_\theta(f)\rangle$ at different radial locations. (right panel) Bicoherency spectrum $b_f(f_1, f_2)$ at the plasma edge ($\Delta r = -2.1$ cm).

ALCATOR scaling. At the plasma edge, the low temperature leads to the relative strong ion-ion collision damping of ZF (according to simulation [5]); as a possible result the flows observed in our experiment are low and their shear is weak. Extended to the parameters of core plasma, one could look for strong ZF, which could contribute significantly to the suppression of turbulence. This is consistent with the experimental observations that higher fluctuations and transport at the plasma edge than at the plasma center.

The ZF generation mechanism has been considered as a three-wave coupling problem in which smaller-scale AT transfer their energy nonlinearly to larger-scale ZF through the RS [3]; the energy is transferred via the inverse cascading of fluctuation spectra. So the process of ZF generation can be investigated using the cross bicoherence $b^2(f) = \sum_{f=f_1+f_2}\langle \tilde{V}_r(f_1)\tilde{V}_\theta(f_2)\tilde{V}^*_\theta(f)\rangle$ [7], namely, that of the radial and poloidal $E \times B$ velocities of the AT with the poloidal $E \times B$ flows, where the $\tilde{V}_r$ and $\tilde{V}_\theta$ were directly measured with the forked probe. The bicoherence spectrum $b_f(f_1, f_2)$ measured at $\Delta r = -2.1$ cm is plotted in Fig. 5 (right). It was computed from 1170 realizations (mean removed) of 512 samples using established techniques [11,22]. We found that to get converged bicoherence spectrum the ensemble with a large number of realizations is necessary; therefore as long as 300 ms records were used. For short record length, the bicoherence spectrum will be dominated by gross feature. In this figure, the degree of phase coupling with $f = f_1 \pm f_2$ is plotted; the $f_2 > 0$ triangle corresponds to sum coupling $f = f_1 + f_2$ and the $f_2 < 0$ region corresponds to difference coupling $f = f_1 - f_2$. Clear structure indicates there existed significant difference frequencies ($f = f_1 - f_2 < 10$ kHz) coupling with the contributing modes (f_1, f_2) both in the AT frequency band (10–200 kHz), and low-frequency flows (<10 kHz) were generated from this three-mode interaction. The integrated bicoherency $b^2(f)$ at different radial locations are plotted in Fig. 5 (left). Identical record length and the number of realizations allow us to compare $b^2(f)$ between different radial locations. In the plasma edge region, a clear low-frequency structure (0–10 kHz) can be seen in the spectra, while very weak coupling in the same frequency region in the SOL. The cross bicoherence of the turbulent RS thus indicates the existence of nonlinear three-wave coupling processes and the generation of low-frequency $E \times B$ flows at the plasma edge. In conclusion, the poloidal long-wavelength $E \times B$ time-varying flows were directly measured using a forked Langmuir probe in the HT-7 tokamak. Nonlinear turbulence simulation [5] has identified distinguishing features of ZF, which are similar to the observations reported here, including its frequency, spatial structure, radial localization, and generation process.

This work was supported by the National Natural Science Foundation of China under Grant No. 10175069.

[1] P. H. Diamond and Y. B. Kim, Phys. Fluids B **3**, 1626 (1991).
[2] K. H. Burrell, Science **281**, 1816 (1998).
[3] P. H. Diamond *et al.*, *Proceedings of the 17th IAEA Fusion Energy Conference, Yokohama, 1998* (IAEA, Vienna, 2001).
[4] P. H. Diamond *et al.*, Phys. Rev. Lett. **72**, 2565 (1994).
[5] Z. Lin *et al.*, Science **281**, 1835 (1998).
[6] T. S. Hahm *et al.*, Plasma Phys. Controlled Fusion **42**, A205 (2000).
[7] P. H. Diamond *et al.*, Phys. Rev. Lett. **84**, 4842 (2000).
[8] Y. H. Xu *et al.*, Phys. Rev. Lett. **84**, 3867 (2000).
[9] S. Coda, M. Porkolab, and K. v. H. Burrell, Phys. Rev. Lett. **86**, 4835 (2001).
[10] G. R. Tynan *et al.*, Phys. Plasmas **8**, 2691 (2001).
[11] R. A. Moyer *et al.*, Phys. Rev. Lett. **87**, 135001 (2001).
[12] M. Jakubowski, R. J. Fonck, and G. R. McKee, Phys. Rev. Lett. **89**, 265003 (2002).
[13] M. G. Shats and W. M. Solomon, Phys. Rev. Lett. **88**, 045001 (2002).
[14] C. Hidalgo *et al.*, Phys. Rev. Lett. **83**, 2203 (1999).
[15] R. A. Moyer *et al.*, Phys. Plasmas **2**, 2397 (1995).
[16] G. S. Xu, B. N. Wan, and M. Song, Phys. Plasmas **9**, 150 (2002).
[17] B. N. Wan *et al.*, Nucl. Fusion **41**, 1835 (2001).
[18] Ch. P. Ritz *et al.*, Rev. Sci. Instrum. **59**, 1739 (1988).
[19] G. S. Xu *et al.*, J. Nucl. Mater. **313–316**, 259 (2003).
[20] B. A. Carreras *et al.*, Phys. Rev. Lett. **80**, 4438 (1998).
[21] B. A. Carreras *et al.*, Phys. Plasmas **5**, 3632 (1998).
[22] Y. C. Kim and E. J. Powers, IEEE Trans. Plasma Sci. **7**, 120 (1979).